

# Numerical Characterization of Shear Elasticity Values Estimated with the Time-of-Flight Approach

Luke M. Wiseman\*, Matthew W. Urban†, and Robert J. McGough\*§

\*Electrical and Computer Engineering, Michigan State University, East Lansing, MI, 48824, [mcgough@egr.msu.edu](mailto:mcgough@egr.msu.edu)

†Department of Radiology, Mayo Clinic, Rochester, MN, 55905

**Abstract**— In clinical ultrasound applications, there is a need for accurate estimates of the shear elasticity, which is directly relevant to the characterization of liver fibrosis, cancer, and other pathologies. The time-of-flight (TOF) approach, which is widely used for estimating the shear elasticity, is effective in purely elastic media, but the TOF approach tends to overestimate the shear elasticity in viscoelastic shear wave phantoms and in soft tissues. To determine the range of shear viscosity values over which the TOF approach yields accurate estimates for the shear elasticity, multiple three-dimensional (3D) simulations of the acoustic radiation force and resulting shear wave particle displacement are assessed. The TOF method is evaluated for values of shear elasticity and shear viscosity within the range of values encountered in healthy liver tissue. A realistic 3D model of the acoustic radiation force is calculated using the fast nearfield method and the angular spectrum approach in FOCUS (<https://www.egr.msu.edu/~fultras-web>), and then the shear waves are simulated in 3D with Green's functions in viscoelastic media on a graphics processing unit (GPU). The TOF method is evaluated within a two-dimensional (2D) cross-section and is based on the Kelvin-Voigt model for a viscoelastic material. The results demonstrate that the accuracy of the TOF method is dependent on the shear elasticity and the shear viscosity, where the accuracy of the TOF method worsens as the shear viscosity increases within the ranges encountered in liver and also worsens as the elasticity increases for a fixed value of shear viscosity.

## I. INTRODUCTION

In shear wave elasticity imaging (SWEI), the mechanical properties of soft tissue are determined by analyzing the shear wave induced by an acoustic radiation force [1], which is useful because mechanical properties are frequently associated with the state of tissue. In SWEI, the shear elasticity is often estimated with the time-of-flight (TOF) method. With the TOF approach, the arrival times for the shear wave are estimated in different lateral positions at the same depth. Although accurate values for the shear elasticity are obtained in elastic (lossless) materials [2, 3], the TOF method produces much larger errors in the shear elasticity when applied to viscoelastic soft tissues [4,5], which suggests that the shear viscosity is responsible for significant bias in the estimated arrival times. Results obtained

when the TOF method is applied to three-dimensional (3D) shear wave simulations indicate that significant errors in the estimated shear elasticity are frequently observed and that the regions where accurate estimates are obtained are often quite small, especially in viscoelastic media.

## II. THEORY

### A. Acoustic Radiation Force

For SWEI measurements of the shear elasticity with the TOF method, an Acoustic Radiation Force (ARF) push beam produces the shear waves in soft tissue with a transducer array that generates one or more focused or unfocused ultrasound beams. The expression  $f(\mathbf{r}, t) = \frac{2\alpha_p I(\mathbf{r}, t)}{c_p}$  describes the acoustic radiation force, where  $f(\mathbf{r}, t)$  is the body force,  $\mathbf{r}$  is an observation point,  $t$  is the time,  $\alpha_p$  is the attenuation,  $c_p$  is the sound speed, and  $I(\mathbf{r}, t) = |p(\mathbf{r}, t)|^2 / (2\rho c_p)$  is the intensity.

### B. Shear Waves in Viscoelastic Media

The Kelvin-Voigt viscosity model applied to Navier's equation [6,7]

$$\left(\lambda + 2\mu + (\eta_p + 2\eta_s) \frac{\partial}{\partial t}\right) \nabla(\nabla \cdot \mathbf{u}) + \left(\mu + \eta_s \frac{\partial}{\partial t}\right) \nabla \times (\nabla \times \mathbf{u}) + \mathbf{f} = \rho \frac{\partial^2 \mathbf{u}}{\partial t^2}, \quad (1)$$

describes shear wave propagation in a viscoelastic medium, where the bulk and shear viscosities are given by  $\eta_p$  and  $\eta_s$ , respectively, and  $\rho$  indicates the density. The 3D simulated shear waves are computed with an approximate Green's function solution [8] to Eq. (1).

## III. METHODS

### A. Shear wave simulations

A realistic simulated 3D acoustic radiation force push, which provides the input to the 3D shear wave simulations, is computed in FOCUS (<http://www.egr.msu.edu/~fultras-web/>) with  $c_p = 1500$  m/s and  $\alpha_p = 0.5$  dB/cm/MHz. A simulated

128-element L7-4 Philips linear ultrasound transducer array (Philips Healthcare, Andover, MA) with a center frequency of 4.09 MHz produces the acoustic radiation force. In the FOCUS simulations, the L7-4 array excites 40 contiguous elements that are focused at  $(x,z) = (0,25)$  mm. The elevation focus of the simulated L7-4 array is located at a depth of 25 mm, the width of each element is 0.283 mm, the height of each element is 7 mm, and the kerf is 0.025 mm. In each simulation, the center of the L7-4 array is located at  $(x,y,z) = (0,0,0)$ . Each transducer element is located on the y-axis, so the normal at the center of the array is coincident with the z-axis. The push beam is evaluated from 0 to 40 mm in the z-direction, -10 to 10 mm in the x-direction, and -5 to 5 mm in the y direction.

Shear wave particle velocities are calculated on eight nVidia (Santa Clara, CA) K80 graphical processing units (GPUs) by convolving the Green's function solution to Eq. (1) both spatially and temporally [8]. In these evaluations, shear wave particle velocities induced by a simulated push beam, which is focused at a depth of 25 mm, are calculated with elastic and viscoelastic simulation models. The shear wave particle displacements are calculated in the xz plane with  $y = 0$ , which ranges from -19.4 mm to 19.4 mm in the x direction and from 0 to 40 mm in the z direction with a spatial increment of 0.154 mm, and the shear wave particle velocities are then obtained. The temporal sampling in these simulations is 155.76  $\mu$ s.

#### IV. RESULTS

With the results obtained from the 3D shear wave simulations, shear elasticity values are estimated using the TOF method.

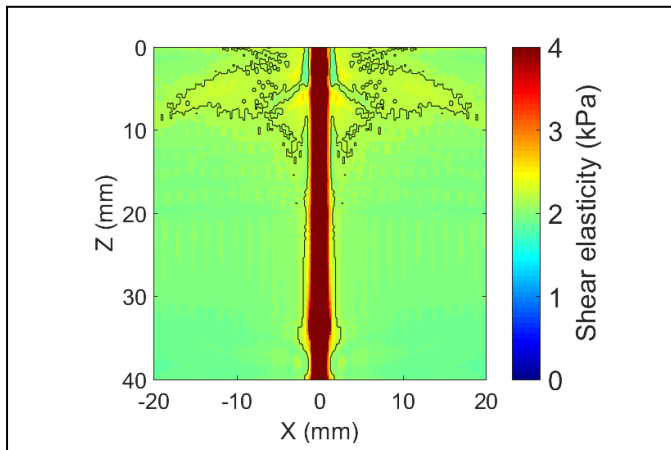


Fig. 1: Estimated values for the shear elasticity obtained from the time-of-flight method applied to 3D simulated shear wave data with shear elasticity  $\mu = 2$  kPa and shear viscosity  $\eta_s = 0.0$  Pa·s. Black contours surround the region where the estimated value is within 10% of the correct value, which covers 80.32% of the area in this figure and is denoted by light green.

Figs. 1-4 show the spatial distribution of estimated values of shear elasticity for 4 different combinations of the simulation parameters. In each figure, the color axis ranges from 0 kPa to twice the forward simulated value of  $\mu$ , and in each forward calculation, the values of  $\mu$  and  $\eta_s$  are constant throughout the

simulated 3D volume. The center of the color axis, which is represented by green, indicates the locations where the TOF method yields estimates for  $\mu$  that are closest to the value applied to the forward simulation. In each figure, a black contour line defines the extent of the region where the estimated value is within 10% of the correct value.

Fig. 1 shows the estimated values of the shear elasticity produced by the TOF method when the shear elasticity  $\mu = 2$  kPa and the shear viscosity  $\eta_s = 0.0$  Pa·s in the forward 3D shear wave simulations. In Fig. 1, a large green region is observed within the black contour lines, which indicates the locations where the estimated  $\mu$  value is within 10% of the correct value. Within Fig. 1, 80.32% of the area evaluated falls within the region defined by the black contour. A dark red vertical region is present in this figure along the z-axis, indicating that the errors in the estimates for  $\mu$  obtained with the TOF method equal and exceed 100% in this region. This result is expected at and near the source of the push beam. The value of  $\mu$  is also slightly overestimated near the top of Fig. 1 where the ultrasound transducer is located.

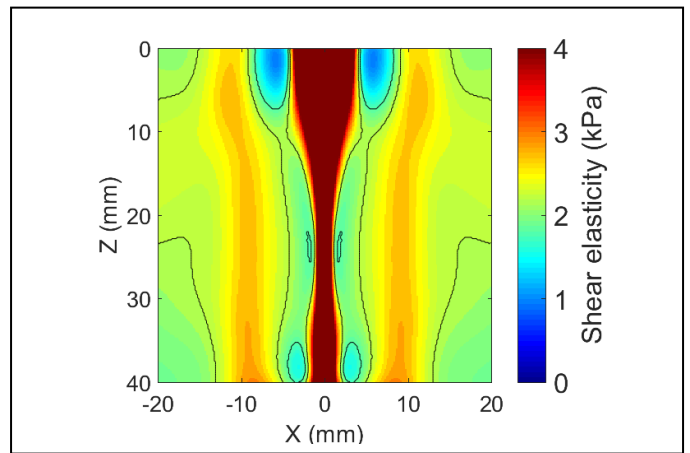


Fig. 2: Estimated values for the shear elasticity obtained from the time-of-flight method applied to 3D simulated shear wave data with shear elasticity  $\mu = 2$  kPa and shear viscosity  $\eta_s = 1.0$  Pa·s. Black contours surround the region where the estimated value is within 10% of the correct value, which covers 26.34% of the area in this figure and is denoted by light green.

Fig. 2 shows the estimated values of the shear elasticity produced by the TOF method applied to 3D shear wave simulations with a  $\mu$  value of 2 kPa and an  $\eta_s$  value of 1.0 Pa·s. The  $\mu$  parameter used in Fig. 2 is the same as in Fig. 1, but  $\eta_s$  is modified so that the 3D shear wave simulations describe the results for a viscoelastic medium. In contrast to Fig. 1, where the majority of the figure has a light green color, a significantly smaller portion of Fig. 2 is contained within the black contour lines. In Fig. 2, 26.34% of the image shown falls within the region of the image where the estimated  $\mu$  value is within 10% of the correct value. As in Fig. 1, a dark red vertical stripe is present along the z-axis in Fig. 2. In addition, large orange vertical regions are also present to the left and right, separated from the central dark red region in Fig. 2 by light green regions that contain small areas of underestimated (light blue) values.

The four corners of Fig. 2 are also contained within the black contour lines; however, the rest of the figure shows a slight bias towards the upper half of the color axis, indicating that the TOF method is calculating overestimated values for  $\mu$  in these regions.

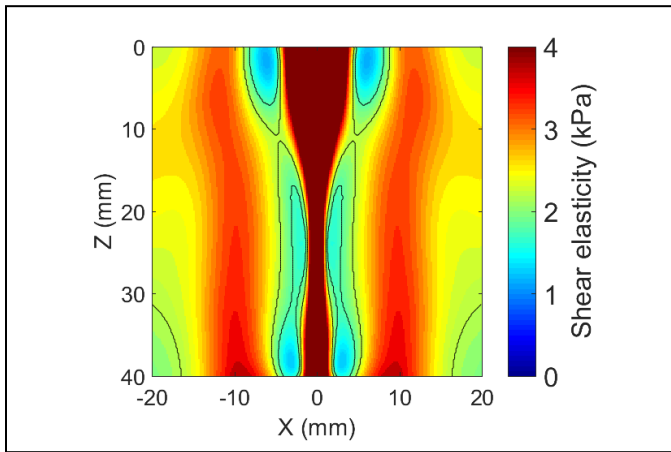


Fig. 3: Spatial distribution of the shear elasticity values estimated with the time-of-flight method obtained from 3D shear wave simulations with a shear elasticity of 2 kPa and shear viscosity of 2.0 Pa·s. Black contours surround the region where the estimated value of  $\mu$  is within 10% of the correct value, which covers only 10.69% of the area in the image shown and is indicated by a light green.

Fig. 3 shows the estimated values of the shear elasticity produced by the TOF method applied to 3D shear wave simulations with a  $\mu$  value of 2 kPa and an  $\eta_s$  value of 2.0 Pa·s. The  $\mu$  parameter used in Fig. 3 is the same as that in Figs. 1-2, but  $\eta_s$  is increased relative to the value used for Fig. 2. Fig. 3 displays the same red regions along the z-axis that are visible in Figs. 1-2, however now the region contained within the black contour lines is even smaller than in Fig. 2, containing only 10.69% of the area evaluated in Fig. 3. Large red and orange vertical regions to the left and right of the z-axis are observed in Fig. 3, although in Fig. 3 these regions are a darker shade that contain colors closer to the upper end of the color axis than in Fig. 2, which indicates that the TOF estimated shear elasticity values in these areas in Fig. 3 contain larger errors than in Fig. 2. The only regions of Fig. 3 that are contained within the black contour lines are at the bottom left and right corners of the figure as well as some small slivers of light green between the large dark red vertical region along the z-axis and the two large dark red regions to the left and right.

Fig. 4 shows the estimated values of the shear elasticity produced by the TOF method applied to 3D shear wave simulations with a  $\mu$  value of 2 kPa and an  $\eta_s$  value of 3.0 Pa·s. The  $\mu$  parameter used in Fig. 4 is the same as in Figs. 1-3, but  $\eta_s$  is increased relative to the value used for Fig. 3. Similar to Figs. 1-3, a large dark red region is present along the z-axis. Fig. 4 also displays the same trend observed in Figs. 2-3, with the percentage of the plot within the black contour lines decreasing to just 5.80% in Fig. 4 along with two large dark red vertical regions that appear to the left and right of the previously mentioned region along the z-axis. In Fig. 4, small

slivers of light green coloration are observed outlining dark blue regions that denote underestimated values for  $\mu$  located between the dark red vertical regions that represent significantly overestimated values for  $\mu$ .

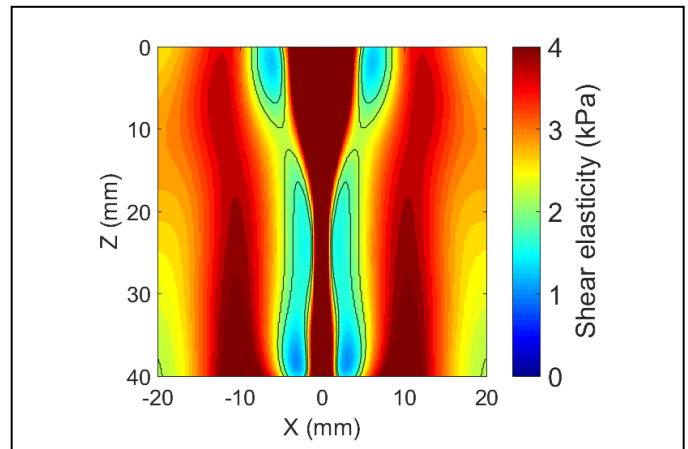


Fig. 4: Estimated values for the shear elasticity obtained from the time-of-flight method applied to 3D simulated shear wave data with shear elasticity  $\mu = 2$  kPa and shear viscosity  $\eta_s = 3.0$  Pa·s. Black contours surround the region where the estimated value is within 10% of the correct value, which covers only 5.80% of the area in this figure and is denoted by light green.

## V. DISCUSSION

### A. Sources of bias in the time-of-flight method

One problem with the TOF method is the implicit plane wave assumption. Most TOF approaches only correlate in the lateral direction, which implicitly assumes that the shear wave propagates only laterally. However, complicated diffraction effects are observed in all shear waves induced by a 3D acoustic radiation force [8]. An additional problem with the TOF method is that different values of the estimated shear elasticity are obtained for various focal depths, transducer types, and lateral ranges applied to the same viscoelastic shear wave phantom [9]. This suggests that diffraction of both the shear wave and the push beam contribute to the bias observed in shear wave parameter estimates obtained from the TOF method.

## VI. CONCLUSION

For elastic media, the TOF method produces images of the shear elasticity that contain accurate values over wide areas. However, when applied to viscoelastic media, the bias produced by the TOF method significantly impacts the estimated shear elasticity, producing less accurate values overall while yielding accurate values in much smaller regions. Since soft tissue is viscoelastic [10], the TOF method is expected to encounter similar difficulties as the viscosity increases. This suggests that alternative methods for SWEI are needed for imaging viscoelastic phantoms and soft tissues. We anticipate that these problems will be solved with optimization-based approaches [8] and other enhanced methods, which are topics of ongoing research.

## ACKNOWLEDGMENTS

This work was supported in part by NIH Grants DK092255, EB012079, and EB023051 and by Michigan State University through computational resources provided by the Institute for Cyber-Enabled Research.

#### REFERENCES

- [1] A. P. Sarvazyan, O. V. Rudenko, S. D. Swanson, J. B. Fowlkes, and S. Y. Emelianov, "Shear wave elasticity imaging: a new ultrasonic technology of medical diagnostics," *Ultrasound in Medicine & Biology*, vol. 24, no. 9, pp. 1419-1435, 1998.
- [2] M. E. Hachemi, S. Callé, and J. Remenieras, "Transient displacement induced in shear wave elastography: comparison between analytical result and ultrasound measurements," *Ultrasonics*, vol. 44, pp. e221-e225, 2006.
- [3] M. I. Hassan, N. M. Salem, and M. I. Eladawy, "A New Shear Wave Speed Estimation Method for Shear Wave Elasticity Imaging," *IEEE Transactions on Ultrasonics, Ferroelectrics, and Frequency Control*, vol. 62, no. 12, pp. 2106-2114, 2015.
- [4] M. Wang, B. Byram, M. Palmeri, N. Rouze, and K. Nightingale, "On the precision of time-of-flight shear wave speed estimation in homogeneous soft solids: initial results using a matrix array transducer," *IEEE Transactions on Ultrasonics, Ferroelectrics, and Frequency Control*, vol. 60, no. 4, pp. 758-770, 2013.
- [5] H. Zhao, P. Song, M. W. Urban, R. R. Kinnick, M. Yin, J. F. Greenleaf, and S. Chen, "Bias Observed in Time-of-Flight Shear Wave Speed Measurements Using Radiation Force of a Focused Ultrasound Beam," *Ultrasound in Medicine & Biology*, vol. 37, no. 11, pp. 1884-1892, 2011.
- [6] J. Bercoff, M. Tanter, M. Muller, and M. Fink, "The role of viscosity in the impulse diffraction field of elastic waves induced by the acoustic radiation force," *IEEE Transactions on Ultrasonics, Ferroelectrics and Frequency Control*, vol. 51, no. 11, pp. 1523-1536, 2004.
- [7] K. Aki and P. G. Richards, *Quantitative Seismology*. Geology (University Science Books): Seismology, University Science Books, 2002.
- [8] Y. Yang, M. Urban, and R. J. McGough, "GPU-based Green's function simulations of shear waves generated by an applied acoustic radiation force in elastic and viscoelastic media," *Physics in Medicine & Biology*, vol. 63, no. 10, 10NT01, 2018.
- [9] M. L. Palmeri, M. H. Wang, J. J. Dahl, K. D. Frinkley, and K. R. Nightingale, "Quantifying hepatic shear modulus in vivo using acoustic radiation force," *Ultrasound in Medicine & Biology*, vol. 34, no. 4, pp. 546-558, 2008.
- [10] M. W. Urban, S. Chen, and J. F. Greenleaf, "Error in estimates of tissue material properties from shear wave dispersion ultrasound vibrometry," *IEEE Transactions on Ultrasonics, Ferroelectrics, and Frequency Control*, vol. 56, no. 4, pp. 748-758, 2009.